Macromolecules
ARTICLE

Macromolecules **2010**, *43*, 4247–4252 **4247**
DOI: 10.1021/ma901670m

Physical Aging of Single Wall Carbon Nanotube Polymer Nanocomposites: Effect of Functionalization of the Nanotube on the Enthalpy Relaxation

Anny L. Flory, T. Ramanathan, and L. Catherine Brinson*

Department of Materials Science and Engineering, Department of Mechanical Engineering, Northwestern University, Evanston, Illinois, 60208

Received August 18, 2009; Revised Manuscript Received February 9, 2010

ABSTRACT: The glass-transition temperature and enthalpy relaxation of nanocomposites synthesized with low loadings of single wall carbon nanotubes (1 wt %) in poly(methylmethacrylate) (PMMA) have been investigated using differential scanning calorimetry (DSC). The results are compared with pure PMMA, and the effect of carbon nanotubes on the mobility of the polymer chain is discussed. Composites have been synthesized with unmodified nanotubes (SWNT/PMMA) as well as with amino-functionalized nanotubes (a-SWNT/PMMA) to provide a better interaction between the nanotube and the host matrix material. It was found that the glass-transition temperature of the unmodified nanocomposite SWNT/PMMA is the same as the neat PMMA ($T_g = 99$ °C). A significant increase of 17 °C in the glass-transition temperature of the modified nanocomposite a-SWNT/PMMA is found when compared with the neat PMMA. Glass-transition results indicate that the presence of a-SWNT in PMMA restricts the segmental motion of the polymer chain. No significant change in activation energy of the enthalpy relaxation process or fragility index of PMMA is observed due to the addition of a-SWNT. However, a large broadening of the enthalpy peak is observed with the incorporation of SWNT in PMMA. This broadening leads to difficulty in the calculation of the activation energy and fragility index of SWNT/PMMA. Enthalpy relaxation behavior during isothermal aging is characterized at the same temperature with respect to the respective glass-transition temperatures of the three samples (at T_g and $T_g - 2$ °C (2 °C lower than the glass-transition temperature of each system)). The equilibrium enthalpy is reached at a shorter aging time in pure PMMA compared with SWNT/PMMA and a-SWNT/PMMA. The results obtained for enthalpy recovery show the signature of the restrictive environment of a-SWNT and SWNT on polymer chain mobility.

1. Introduction

The incorporation of nanoparticles in polymers offers a simple way to reinforce thermal, electrical, and mechanical properties of the pure polymers.[1−4] In particular, many investigations reveal that one of the most important properties for the engineering application of polymers, the glass-transition temperature (T_g), can be largely influenced by the incorporation of nanoparticles in the polymer matrix. The nanosize of the particles leads to vast surface areas of polymer−nanoparticle interfaces in the nanocomposite, even at low weight fraction loadings (e.g., 1 wt % or less). Substantial changes in T_g have been reported[5−12] depending on the nature of the polymer−nanoparticle interaction because of alteration of the mobility of the polymer chains in the interphase zones extending from the interfaces.

The long-time performance of polymers is another important property for engineering applications. However, the relaxation process that occurs in the glassy state limits the stability of these materials. This relaxation process is a result of the nonequilibrium state of the polymer below the glass-transition temperature. In fact, because glasses are inherently nonequilibrium materials, their physical and mechanical properties evolve with time as the material attempts to reach the equilibrium state through configurational rearrangement of polymer segments. This is referred to as structural relaxation or physical aging.[13,14] A transition from ductile to brittle mode of failure is observed when a material physically ages.[14] Consequently, characterization of physical aging is of essential importance for polymer engineering. To the best of our knowledge, only a few reports on physical aging of polymer nanocomposites have been published. Similar to the effect on T_g, it was found that the presence of interphases in nanocomposites could influence the physical aging or long-time performance of the material.[6,15−18] These observations were made on various nanocomposites systems, layered silicate-epoxy,[6] layered silicate-polyamide 6,[16] both poly(2-vinyl pyridine)-silica and -alumina,[17] and polymethylmethacrylate-silica[18] using various characterization techniques (differential scanning calorimetry (DSC), creep, fluorescence, dielectric). However, no systematic study that addresses the effect of dispersion and percolation on the physical aging behavior in carbon nanotube polymer nanocomposites has been reported.

In addition to the glass-transition temperature and physical aging behavior, characterization of the dependence of the material properties on temperature in the glass-transition temperature range is very important. Behavior near T_g is critical not only for high-temperature applications of polymers but more generally for polymer processing. The concept of the fragility index, m, which was introduced by Angell,[19−21] provides a classification of the material as a function of its strength to resist property changes in the vicinity of the glass-transition temperature. In this definition, a strong glass former (low m) exhibits low temperature dependence at the liquid-glass transition. Knowledge of the effect

*Corresponding author. E-mail cbrinson@northwestern.edu.

Published on Web 04/09/2010

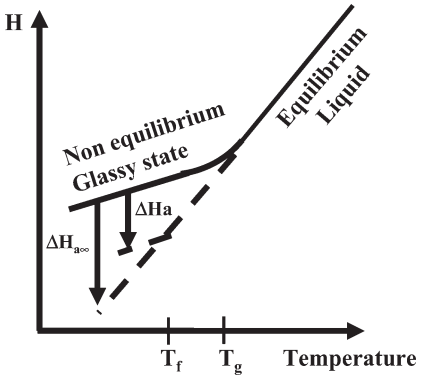

Figure 1. Schematic of enthalpy versus temperature for glass formers.

of interphases on the fragility index is of importance for improving the processing of polymer nanocomposites.

Carbon nanotubes, both single wall (SWNT) and multiwall (MWNT), have attracted great interest in the past decade because of the enhancement of electrical and mechanical properties found when adding small amounts of nanotubes to the polymer. In particular, when the nanotubes are chemically functionalized to make them more compatible with the polymer matrix, a better dispersion of the nanoparticles is achieved, resulting in greater improvement of the material properties.[7,22,23] In this work, we use DSC to study glass-transition behavior, enthalpy relaxation during physical aging, and fragility of an important thermoplastic material (PMMA) in which a low weight fraction (1%) of unmodified nanotubes (SWNT/PMMA) or amino-functionalized nanotubes (aSWNT/PMMA) has been added.

2. Theoretical Background

In this section, we introduce the fundamental relationships used to analyze the experimental data on the nanocomposites obtained by DSC.

2.1. Isothermal Enthalpy Relaxation: TNM/KAHR Model. The Tool−Narayanaswamy−Moynihan (TNM)/Kovacs−Aklonis−Hutchinson−Ramos (KAHR) model[24,25] provides a representation of the enthalpic departure from equilibrium, δ_h. After a temperature jump, the model predicts that during isothermal aging δ_h varies as follows

$$\delta_h = \Delta H_{a\infty} - \Delta H_a(t) = \delta_{h0} \exp\left\{-\left(\int_0^t \frac{dt}{\tau_0}\right)^{\beta}\right\} \quad (1)$$

where $\Delta H_{a\infty}$ is the equilibrium enthalpy loss (Figure 1), $\Delta H_a(t)$ is the enthalpy loss at aging time t, δ_{h0} is the initial enthalpic departure from equilibrium ($\Delta H_{a\infty} = \delta_{h0}$), and β is the nonexponentiality parameter (or stretching parameter) in the Kohlrausch−William−Watts function (KWW).[26] The characteristic relaxation time (τ_0) of the glass depends on both the temperature (T) and the instantaneous structure of the glass[27] (which is represented by the fictive temperature (T_f), Figure 1)

$$\ln \tau_0 = \ln A + \frac{\Delta h}{RT} + \frac{(1-x)\Delta h}{RT_f} \quad (2)$$

where A is the pre-exponential factor, Δh is the apparent activation energy, R is the gas constant, x is the nonlinearity parameter, and T_f is the fictive temperature, which is related to δ_h by

$$T_f = T_a + \frac{\delta_h}{\Delta C_p} \quad (3a)$$

where T_a is the aging temperature and ΔC_p is the change in the heat capacity at the glass-transition temperature.

Equation 3a arises from general relation

$$\Delta H = \int \Delta C_p \, dT \quad (3b)$$

Equations 1 through 3a can be solved numerically to predict the time evolution of the fictive temperature. Note that there are four independent parameters in this model: Δh, x, ln A and β.

Experimentally, Δh can be determined from the dependence of T_f on the cooling rate in enthalpy relaxation experiments, x from the peak shift method[28] using isothermal annealing experiments, ln A from Δh and T_g at a given cooling rate, and β can be estimated from structural recovery obtained in linear temperature jump experiments.

2.2. Strength of the Glass Former at T_g: Fragility Index. The fragility index, m, of the glass[19] is used to determine the stability of the structure and of dynamics and thermodynamic properties of the glass in the glass-transition temperature range. Strong glasses have a lower fragility index, reflecting a low dependence of the physical and mechanical properties on the temperature in the vicinity of T_g. The index is defined as

$$m = \Delta h/(2.302RT_g) \quad (4)$$

where all variables are previously defined. For a description of the measuring nonlinearity and activation energy, see the Experimental Methods section.

3. Experimental Methods

3.1. Materials Preparation. The materials studied in this work are PMMA, SWNT/PMMA, and a-SWNT/PMMA. The poly(methylmethacrylate) (PMMA) was obtained from Poly-Sciences. It has a weight-average molecular weight of 350 000 g/mol and a polydispersity index of 1.15. Purified HiPCO SWNTs (Bucky Pearls) were supplied by Carbon Nanotechnologies, Inc. SWNTs were amino-functionalized (a-SWNT) to provide a better interaction with PMMA matrix. Details of the amino-functionalization of SWNT can be found elsewhere[7] and consist of chemical oxidation of the nanotube, followed by direct coupling of ethylene diamine.

The nanocomposites were prepared by a solution evaporation technique following the steps:[7] (1) dissolution of PMMA in tetrahydrofuran (THF); (2) dispersion of SWNT (1 wt %) in THF and bath sonication of the solution for 1 h; (3) addition of PMMA solution in SWNT solution and sonication of the mixture for 1 h; (4) precipitation of the mixture in methanol and filtration of the precipitate using a polytetrafluoroethylene filter paper with a pore size of 10 μm; (5) solvent evaporation (mixture is dried and placed under vacuum at 80 °C for 10 h); and (6) material (SWNTPMMA) is hot-pressed at 210 °C and 200 Pa for 10 min

The same procedure is followed to prepare the a-SWNT/PMMA sample. However, in this case, an additional step is taken between steps 3 and 4. After sonication, the mixture of a-SWNT and PMMA was stirred at 60 °C for 5 h and then cooled to room temperature before being precipitated and filtered (step 4). This additional step ensures the formation of covalent bonds between a-SWNT and PMMA.

3.2. Isothermal Enthalpy Relaxation: Enthalpy Overshoot and Nonlinear Parameter. The enthalpy recovery experiments were carried out on a Mettler-Toledo differential scanning calorimetor equipped with a refrigerated cooling system. All experiments were performed under a nitrogen atmosphere. The instrument was calibrated using a metal standard (indium) at 10 and 40 °C/min. A single sample of each material studied, PMMA, SWNT/PMMA,

and a-SWNT/PMMA, was used for all DSC experiments. Another set of samples was used for replicate analysis, providing a check of the variability in the measurement. All samples weighed between 8 and 9 mg, and each was sealed in an aluminum pan. The glass-transition temperatures (T_g) were measured on cooling at a rate of 10 °C/min.

The evolution of the enthalpy, $\Delta H_a(t)$, during isothermal annealing cannot be measured directly in conventional DSC because of the small size of the sample.[14] Instead, the enthalpy relaxation at aging time, t_a, is observed experimentally as the development of an overshoot peak in the heat flow or heat capacity during heating the sample from the aging temperature, T_a, to the equilibrium line. As the time of aging increases, the peak increases and shifts to higher temperatures because of the increase in the relaxation time with aging. The equilibrium liquid line is achieved when the overshoot stops evolving.[29] A procedure similar to the one described by Simon et al.[30] is used in this work to determine structural recovery. In this procedure, the sample is first heated above T_g for 4 min to erase any previous thermal history. The sample was then cooled to the aging temperature (T_a), below T_g, at 40 °C/min and held isothermally for a specific aging time (t_a) ranging from 20 min to 72 h. After aging, the sample was cooled to 30 °C at 40 °C/min and then heated from 30 °C to above T_g at 10 °C/min. This heating ramp constitutes the aged scan (ΔH_a). Following the aged scan, the sample was cooled to 30 °C at 40 °C/min and then immediately heated at 10 °C/min from 30 °C to above T_g. This heating ramp constitutes the unaged scan (ΔH_{unaged}). The change in enthalpy during physical aging is given by the difference between the aged and unaged scans

$$\Delta H = \Delta H_a - \Delta H_{unaged} \quad (5)$$

If the glass were hypothetically heated so that it followed the line parallel to the cooling line, then it would intercept the equilibrium line at a temperature T_f, the fictive temperature. In the case of the unaged scan, the fictive temperature is equal to the glass-transition temperature ($T_f = T_g$). T_f is represented in Figure 1 as the intersection of the glassy enthalpy line and extrapolated liquid line and has been used to describe the instantaneous structure of glasses. When the material is at equilibrium, the fictive temperature is the same as the aging temperature; that is, $T_f = T_a$. In this work, T_f is determined from the DSC heating scan (aged scan) using the equal area method described by Moynihan.[31] The following integral form is applied in this method

$$\int_{T^*}^{T_f'} (C_{p_e} - C_{p_g})\, dT_f = \int_{T^*}^{T'} (C_p - C_{p_g})\, dT \quad (6)$$

where T^* is any arbitrary temperature above the transition region at which the heat capacity is equal to the equilibrium heat capacity, C_{p_e} and C_{p_g} are the heat capacities of the liquid and the glass, respectively, and T' is a temperature well below the transition region. Graphically, T_f can be found by setting T_f to be the T_f' in eq 6 such that the areas related to the C_p curve for the two sides of eq 6 balance.

The nonlinearity parameter, x, which partitions the dependence of τ_0 between the temperature and the fictive temperature, can be obtained from the enthalpy loss obtained during isothermal aging using the peak shift method.[28] The dimensionless peak shift can be defined as

$$\hat{S} = \Delta C_p \left[\frac{\partial T_\rho}{\partial \Delta H_a}\right] \quad (7)$$

here T_ρ is the temperature of the overshoot peak and ΔC_p is the change in the heat capacity at the glass-transition temperature attained by extrapolating the asymptotic glassy and liquid C_p lines to the T_g ($\Delta C_p = C_{p_{liquid}}(T_g) - C_{p_{glass}}(T_g)$). T_ρ and ΔH_a are determined from the C_p curves upon heating after isothermal aging. The data for ΔH_a and T_ρ are plotted; then, the slope is multiplied by ΔC_p to yield the peak shift in 7. The dimensionless peak shift, $\hat{S}$, is strongly dependent on the nonlinear parameter, x, and independent of relaxation time. The master curve of $\hat{S}$ as a function of x has been determined theoretically for various polymer systems,[28] and based on $\hat{S}$, the nonlinear parameter, x, is determined. A small value of x indicates a large nonlinearity, that is, large dependence of the relaxation process on the structure of the glass.

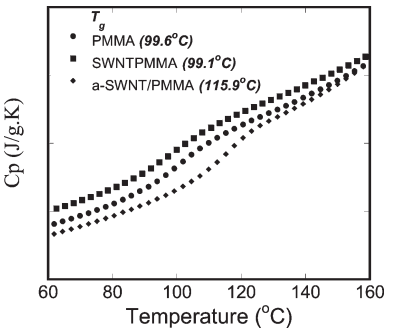

Figure 2. DSC scans of the heat capacity versus temperatures for PMMA, SWNT/PMMA. and a-SWNT/PMMA. T_g is defined from the break in the C_p break (midpoint). It is 99 °C for PMMA and SWNT/PMMA and 116 °C for a-SWNT/PMMA.

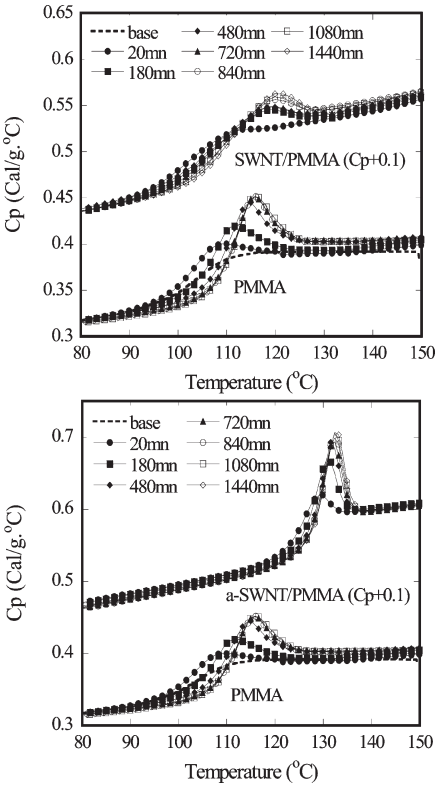

Figure 3. DSC scans of the heat capacity versus temperatures for PMMA, SWNT/PMMA, and a-SWNT/PMMA after isothermal annealing at the respective T_g for various aging times.

3.3. Enthalpy Relaxation under Cooling: Apparent Activation. The cooling rate dependence of the fictive temperature provides a measure of the apparent activation energy (Δh) of the enthalpy relaxation process.[32] A slower cooling rate leads to the formation of a denser glass that will approach equilibrium over a longer time when heated to above the glass-transition temperature

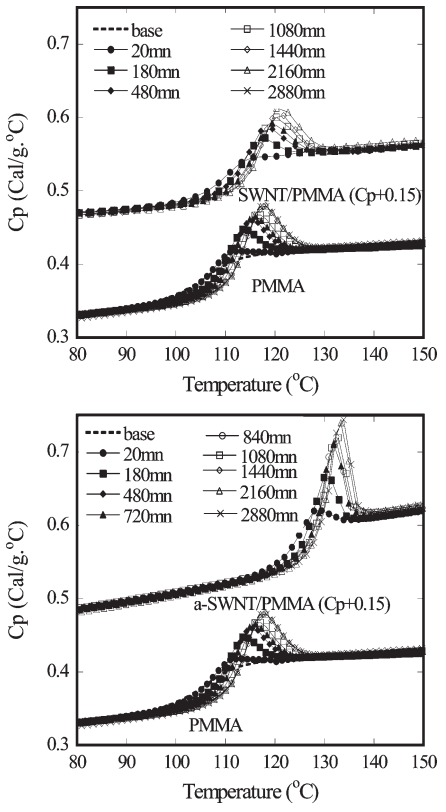

Figure 4. DSC scans of the heat capacity versus temperatures for PMMA, SWNT/PMMA, and a-SWNT/PMMA after isothermal annealing at $T_g - 2$ °C for various aging times.

(larger C_p overshoot). Δh can be obtained from the Ritland−Bartenev equation[32]

$$\frac{\Delta h}{R} = -\frac{d(\ln|q_1|)}{d(1/T_f)} \quad (8)$$

where q_1 is the cooling rate. The heating scans for C_p provide T_f for each cooling rate, q_1. These data points can be plotted so that the slope provides the right-hand side of eq 8 and therefore Δh.

4. Results

4.1. Glass-Transition Temperature. The samples were first annealed at 160 °C for 4 min in the DSC oven to remove residual stresses caused by processing. The glass-transition temperatures were then determined on cooling from 160 °C to the ambient temperature at a rate of 10 °C/min. The heat capacity (C_p) scans collected during cooling are presented in Figure 2 for PMMA, SWNT/PMMA, and a-SWNT/PMMA. The glass-transition temperatures were defined from the break in C_p curve (midpoint). The T_g is 99 °C for both PMMA and SWNT/PMMA, and it is 17 °C higher for a-SWNT/PMMA (116 °C).

4.2. Isothermal Enthalpy Relaxation. *4.2.1. Evolution of C_p Peak−Change in Enthalpy during Aging.* Change in enthalpy is measured during aging at a fixed temperature from the glass-transition temperatures of the different materials. Temperatures T_g and $T_g - 2$ °C are selected in the study. The C_p overshoots at T_g and $T_g - 2$ °C from the respective T_g values of the three samples are plotted in Figures 3 and 4, respectively, for different aging times. In the case of PMMA, the equilibrium in enthalpy relaxation is reached at 720 min at T_g, as evidenced by the stationary C_p overshoot for aging times >720 min (840 and 1080 min). For both nanocomposite materials, SWNT/PMMA and a-SWNT/PMMA, the equilibrium enthalpy is reached at times >720 min as the C_p peaks continue to evolve after aging time of 1440 min. At $T_g - 2$ °C, the equilibrium enthalpy is reached at 840 min for the PMMA sample, whereas the results indicate that the nanocomposites have not reached the equilibrium enthalpy on the same time scale.

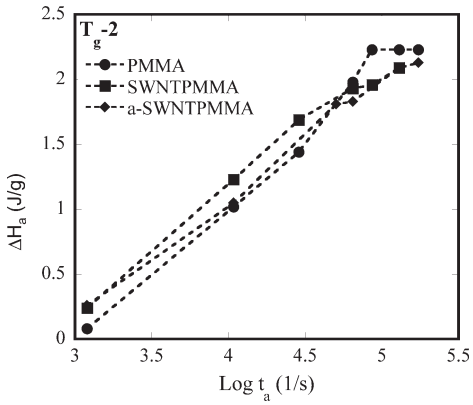

Figure 5. Change in enthalpy versus log aging time for PMMA, SWNT/PMMA, and a-SWNT/PMMA at $T_g - 2$ °C. Dashed lines shown to guide the eye.

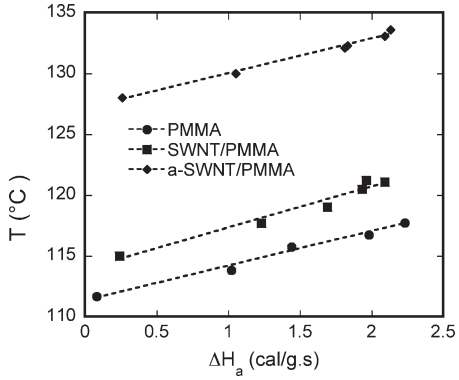

Figure 6. Temperature of the C_p peak versus enthalpy.

The enthalpy value, ΔH, is obtained by integration of the C_p overshoot and removing the enthalpic contribution of the unaged sample (eq 5). The results for the different samples at $T_g - 2$ °C are plotted in Figure 5 for the different aging times.

4.2.2. Nonlinearity Parameter. Equation 7 is used to determine the peak shift $\hat{S}$ and then the nonlinearity parameter, x, from the evolution of the heat capacity at $T_g - 2$ °C, which was presented above. The difference in heat capacity at the glass-transition temperature, ΔC_p, T_ρ, and ΔH_a are determined for each aging time, and the latter two are plotted in Figure 6. The slopes of these data are used to find $\hat{S}$ from eq 7, and then x is found from theoretical calculations developed by Hutchinson.[28] Table 1 shows that the nonlinearity parameter is the same for PMMA, SWNT/PMMA, and a-SWMT/PMMA, which indicates that the dependence of the relaxation time on the structure of the glass is not affected by the inclusion of the nanotubes in PMMA. It should be noted that in this calculation, it is assumed that the theoretical calculations developed for pure glasses[28] are valid for carbon nanotube polymer nanocomposites.

4.3. Effect of Cooling Rate on the Enthalpy Recovery: Activation Energy. Nonisothermal annealing experiments at different cooling rates are performed to obtain the activation energy from eq 8. The C_p scans collected on heating are plotted in Figure 7. As expected, the C_p peak is larger for glasses formed at lower cooling rates because these glasses

Table 1. Difference in Heat Capacity, ΔC_p, at T_g, Dimensionless Peak Shift, and Nonlinearity Parameter, x

	ΔC_p	$\hat{S}$	x
PMMA	0.18	0.50	0.6
SWNT/PMMA	0.15	0.51	0.6
a-SWNT/PMMA	0.20	0.58	0.6

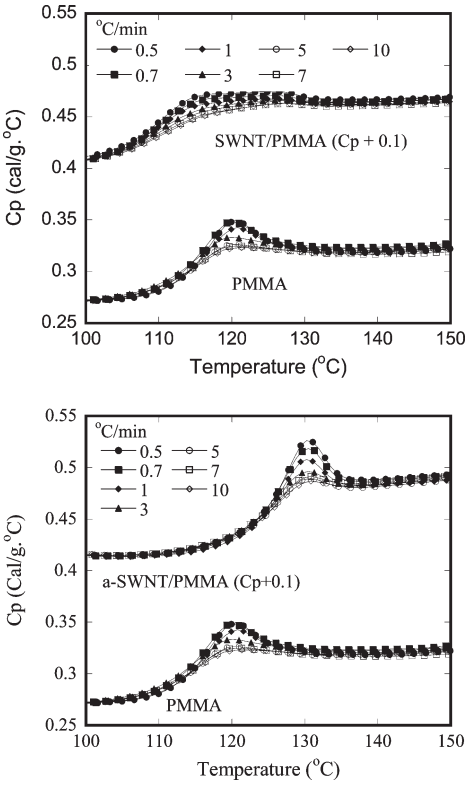

Figure 7. DSC scans of the heat capacity versus temperatures for PMMA, SWNT/PMMA, and a-SWNT/PMMA at various cooling rates. The samples were reheated immediately after being cooled to 80 °C. DSC scans are collected on heating.

have higher density. The fictive temperature is obtained from the C_p scan using the equal peak area method (eq 6). The activation energy is given by eq 8 using the slope of the logarithm of cooling rate as a function of the reciprocal fictive temperature. The results plotted in Figure 8 indicate that the activation energy, $\Delta h/R$, is 147 Kk for PMMA and 130 Kk for a-SWNT/PMMA. The difference in activation energy of the two materials is within the error in the determination of the fictive temperature. The activation energy of SWNT/PMMA is found to be 90 Kk, which is significantly low compared with that of pure PMMA. However, the significant broadening of the C_p peak of SWNT/PMMA (Figure 7) leads to a large uncertainty in the determination of the fictive temperature. Therefore, no conclusion can be made in this study concerning the effect of SWNTs on the value of the activation energy of PMMA.

It is interesting to note that broadening of the relaxation modulus of SWNT/PMMA was observed by Ramanathan et al[3] and was identified as signifying poorer dispersion of unmodified SWNTs in PMMA matrix compared with dispersion of a-SWNT. Therefore, is it possible that the broadening of the C_p curves observed here in the cooling rate experiments are also a signature of poor dispersion of SWNTs (Figure 7)? Further investigation is warranted with a goal to use DSC experiments as straightforward and fast qualitative probe of dispersion of nanoparticles in polymer nanocomposites.

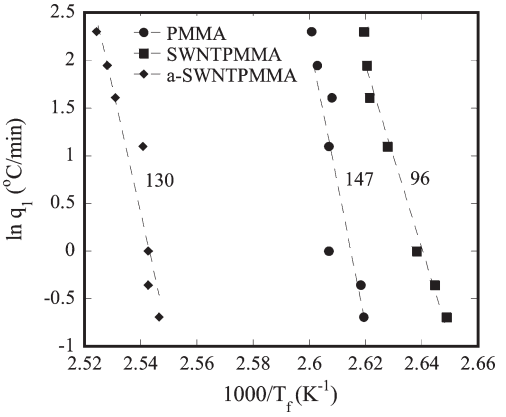

Figure 8. Logarithmic cooling rate as a function of the reciprocal fictive temperature. Values of $\Delta h/R$ (kK) are given by the slope of the lines.

Table 2. Fragility Index, m, for PMMA and a-SWNT/PMMA

	x	$\Delta h/R$ (kK)	T_g (K)	m
PMMA	0.6	146	372	102
SWNT/PMMA	0.6	96	372	NA
a-SWNT/PMMA	0.6	130	389	98

4.4. Fragility Index. The fragility index, m, of PMMA, SWNT/PMMA, and a-SWNT/PMMA are calculated using eq 4 and values of the nonlinearity parameter, activation energy, and T_g determined in previous sections. These values are summarized in Table 2. It is found that PMMA and a-SWNT/PMMA have similar fragility index, indicating that the presence of a-SWNT in PMMA does not influence the dependence of the physical and mechanical properties on temperature in the vicinity of the glass-transition temperature. The fragility index of SWNT/PMMA nanocomposite is not determined because of the uncertainty in the activation energy value, as mentioned previously.

5. Discussion

The results presented here demonstrate that the presence of very small amounts (1%wt) of a-SWNT alters the molecular motions associated with glass-transition and physical aging of PMMA. The results are consistent with previous reports on the same nanocomposite material, where T_g measured by mechanical testing was >20 °C higher than that of neat PMMA,[3] and T_g at the interface between PMMA and a-SWNT was found to be substantially higher when characterized by fluorescence technique.[17,18] Signature of the restriction of the polymer chains with the presence of a-SWNTs is also present in isothermal enthalpy relaxation. The data show that the extent of aging is in fact reduced by the presence of a-SWNTs. Examination of the enthalpy relaxation process from cooling experiments reveals that the addition of a-SWNT in the PMMA matrix does not significantly change activation energy and fragility of the polymer.

The DSC results show no change in the glass-transition temperature of SWNT/PMMA when compared with pure PMMA, and these results are again consistent with previous mechanical testing data.[3] However, relaxation of the polymer chain in the glassy state seems to be affected by the presence of SWNTs because the extent of aging is reduced. A large broadening of the enthalpy relaxation peak of SWNT/PMMA is observed here, potentially related to a broadening of the modulus peak of SWNT/PMMA previously reported.[3] Broadening of these peaks can both be explained by a conflicting effect between areas of both low polymer mobility (at local regions with strong PMMA−SWNT interface) and high polymer mobility (at local regions of weaker PMMA−SWNT interface that may occur at

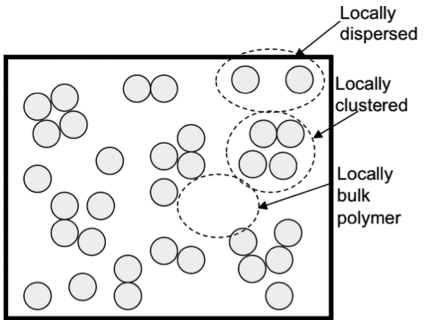

Figure 9. Schematic representing nanoparticle distribution in a nanocomposite system.

SWNT clusters). A schematic of the nanocomposite system with good and poor dispersions is represented in Figure 9. In this schematic, it is noted where local strong interactions may occur and where local SWNT clustering may indicate poor SWNT−PMMA interactions. In the latter case, the clusters may be more poorly wetted with polymer and therefore have polymer of locally higher free volume and hence higher molecular mobility. Such a distribution of polymer mobilities through the sample would lead to broadening of both the C_p peak and the relaxation modulus peaks. Additionally, it is possible that the locally clustered nanotubes result in a different transfer of thermal energy in the material. Therefore, the more poorly dispersed nanocomposite contains a distribution of temperatures in local regions: locally polymer rich regions, locally well-dispersed SWNT regions, and locally clustered SWNT regions. Again, this distribution of thermal transfer would lead to a broadening of the C_p traces, Consequently, enthalpy relaxation cooling experiments may provide an attractive and simple method for dispersion studies.

Whereas the broadening of the C_p peak in the SWNT/PMMA composites illustrates altered mechanisms at play due to the presence of the SWNTs and the broadening may be an indicator of poorer dispersion, at the same time the broad peak leads to difficulty in applying the Moynihan method for the determination of T_f from eq 6. Therefore, there are errors involved in the calculation of the activation energy and the fragility index because T_f is used in these calculations.

6. Conclusions

The DSC results on glass transition of PMMA, SWNT/PMMA, and a-SWNT/PMMA are in good agreement with mechanical testing results reported previously. When very small amounts (1 wt %) of amino-functionalized SWNTs (a-SWNTs) are added to PMMA, the glass transition increases substantially (17 °C). Also, here we found that the extent of physical aging is significantly decreased in a-SWNT/PMMA compared with neat PMMA. At the same time, the study shows that the activation energy of the relaxation process and the fragility index in PMMA and a-SWNT/PMMA are comparable within the experimental error.

When SWNTs are incorporated in the PMMA matrix without being functionalized, no change in the glass-transition temperature is observed. However, aging experiments also indicate a slower approach to equilibrium compared with neat PMMA, signifying a reduced aging rate in these nanocomposite systems. Additionally, a significant broadening in the C_p peak is observed, which we argue indicates a poorer dispersion of SWNT in PMMA. The possibility that DSC could be used as a probe of dispersion of nanoparticles in polymer matrices is currently under investigation.

Although the results here show slower approaches to equilibrium for both functionalized and unfunctionalized nanotubes in PMMA, it is important to note the uncertainty in the activation energy of SWNT/PMMA systems due to broadening in the C_p peak. For the functionalized system, a-SWNT-PMMA, the homogeneous dispersion results in direct comparison between the nanocomposites and the neat PMMA and definitively indicates that both higher glass transition and dramatically reduced aging rate can be attained in such systems.

References and Notes

(1) Rao, A. *Science* **1997**, *275*, 187–191.
(2) Ajayan, P. *Adv. Mater*. **2000**, *12*, 750–753.
(3) Ramanathan, T.; Fisher, F. T.; Ruoff, R. S.; Brinson, L. C. *Chem. Mater*. **2005**, *17*, 1290.
(4) Etienne, S. *J. Therm. Anal. Calorim*. **2007**, *87*, 2007.
(5) Via, R. A. *J. Polym. Sci., Part B: Polym. Phys*. **1997**, *35*, 59–67.
(6) Lu, H. *Macromol. Chem. Phys*. **2003**, *204*, 1832–1841.
(7) Ramanathan, T. *J. Polym. Sci., Part B: Polym. Phys*. **2005**, *43*, 2269–2279.
(8) Gonzales-Irun Rodriguez, J. *J. Therm. Anal. Calorim*. **2007**, *87*, 45–47.
(9) Schandler, L. S. *JOM* **2007**, *59*, 53–60.
(10) Lopez-Martinez, E. l. *J. Polym. Sci., Part B: Polym. Phys*. **2007**, *45*, 511–518.
(11) Rodriguez, J. G. I. *J. Therm. Anal. Calorim*. **2007**, *87*, 45–47.
(12) Jia, Q. *Eur. Polym. J*. **2007**, *43*, 35–42.
(13) Struik, L. C. E. *Physical Ageing in Amorphous Polymers*; Elsevier: Amsterdam, 1978.
(14) Simon, S. L. In *Encyclopedia of Polymer Science and Technology*; Mark, H. F., Ed.; John Wiley & Sons: Hoboken, NJ, 2002.
(15) Lu, H. B.; Nutt, S. *Macromolecules* **2003**, *36*, 4010–4016.
(16) Vlasveld, D. P. N. *Polymer* **2005**, *46*, 12539–12545.
(17) Rittigstein, P. *J. Polym. Sci., Part B: Polym. Phys*. **2006**, *44*, 2935–2943.
(18) Priestley, R. D. *J. Phys.: Condensed Matter* **2007**, *19*, 205120.
(19) Angell, C. A. *J. Non-Cryst. Solids* **1991**, *13*, 131–133.
(20) Angell, C. A. *Science* **1995**, *67*, 1924.
(21) Angell, C. A. *J. Res. Nat. Inst. Std. Technol*. **1997**, *102*, 171.
(22) Mitchell, C. A.; Bahr, J. L.; Arepalli, S.; Tour, J. M.; Krishnamoorti, R. *Macromolecules* **2002**, *35*, 8825–8830.
(23) Zhu, J.; Kim, J.; Peng, H.; Margrave, J. L.; Khabashesku, V. N.; Barrera, E. V. *Nano Lett*. **2003**, *3*, 1107–1113.
(24) Tool, A. Q. *J. Am. Ceram. Soc*. **1931**, *14*, 276–308.
(25) Kovacs, A. J. *J. Polym. Sci., Polym. Phys. Ed*. **1979**, *17*, 1097–1162.
(26) Williams, G. *Trans. Faraday Soc*. **1970**, *66*, 80.
(27) Narayanaswamy, O. S. *J. Am. Ceram. Soc*. **1971**, *54*, 491–498.
(28) Hutchinson, J. M. *J. Polym. Sci., Part B: Polym. Phys*. **1988**, *26*, 2341.
(29) Li, Q. *Polymer* **2006**, *47*, 4781–4788.
(30) Echeverria, I. *J. Polym. Sci., Part B: Polym. Phys*. **1995**, *33*, 2457–2468.
(31) Moynihan, C. T. In *Assignment of the Glass Transition*; Seyler, R. J., Ed.; American Society for Testing Materials (ASTM): Philadelphia, PA, 1994.
(32) Ritland, J. *J. Am. Ceram. Soc*. **1956**, *39*, 403.